# Modeling and Optimization of an Industrial Glass Furnace

M. G. Carvalho, P. Oliviera, and V. Semião

# Modeling and Optimization of an Industrial Glass Furnace

M. G. Carvalho,* P. Oliveira,† and V. Semião‡
*Instituto Superior Técnico, Lisbon, Portugal*

## Abstract

A mathematical model for the prediction of the performance of an industrial glass furnace is described. It comprises submodels for the combustion chamber and the glass tank flow. The first submodel incorporates physical modeling for the turbulent diffusion flame, soot formation and consumption, and thermal radiation. The second submodel incorporates physical modeling for the laminar flow and energy balance of the molten glass, driven by free convection. The PISO algorithm is used in this submodel to solve the finite-difference equations. The whole mathematical model is applied to a cross-fired regenerative furnace. An iterative procedure is used, where the heat transfer to the upper surface of the molten glass is that calculated for the combustion chamber, by the first submodel, assuming known values of the temperature of the referred surface. These temperatures are calculated by the second submodel using as a boundary condition the heat transfer fluxes calculated by the first submodel. The whole procedure is repeated until "convergence" is achieved. Predictions are made for an extensive range of parameters showing the abilities of the present procedure as a tool to improve industrial glass furnaces designs and operating conditions.

---

* Associate Professor, Mechanical Engineering Department
† Research Assistant, Mechanical Engineering Department
Present affiliation: Research Assistant, Mineral Resources Engineering Department, Imperial College, London
‡ Research Assistant, Mechanical Engineering Department

### Nomenclature

$g_i$    = gravitational acceleration in the i-direction

$K_{eff}$    = effective thermal conductivity of the glass

$p$    = pressure

$S_T$    = source term of temperature equation

$T$    = temperature

$u_i$    = velocity component in the i-direction

$x_j$    = co-ordinate direction

$\Gamma_T$    = molecular exchange coefficient for temperature

$\delta_{ij}$    = Kronecker's delta

$\mu$    = molecular viscosity

$\rho$    = time-mean density

## I.   Introduction

### A. Preamble

The recent awareness of the limitation of energy resources, the increase in fuel prices, and the problem of pollution have turned the combustion engineers' attention toward the importance of improving the combustion equipment design.

There is currently considerable interest from the glass and ceramic industry to support the construction of a mathematical model that reliably simulates the performance of the glass melting furnaces. Glass furnaces are large and are thus extremely costly to develop by highly empirical methods.

Most of the previous glass furnace predictive studies have avoided the complexities of the combustion chamber region and have confined their attention to the flow in the tank [see Chen and Goodson (1972), Suzuki (1976), and Oliveira (1986), for example].

A three-dimensional simulation of a glass furnace combustion chamber in which the flowfield and heat release were determined from a numerical solution of the governing balance equations was presented by Gosman et al. (1980). The works of Carvalho (1983) and Semião (1986) have extended the work of Gosman et al. (1980) to more complex geometries with a horseshoe flow shape. The predictions of Semião (1986) were made to oxygen-rich burning conditions. The work of

Carvalho et al. (1987) is an extension of Semião (1986) in which the authors have used a two-dimensional axisymmetric model to simulate the burner region providing with these results the inlet conditions for the three-dimensional calculations of the combustion chamber. The results were extensively validated with experimental data acquired in the referred furnace (Carvalho et al. 1988-a).

There have been very few attempts to model a complete glass furnace. A simplified model was presented by McConnell and Goodson (1979) in which global energy equations for the combustion chamber, molten glass, and feed ("batch") were solved for an assumed flow and heat release, with Hottel's zone method employed to calculate the combustion chamber radiation. A similar study was effected by Mase and Oda (1980), but the flowfield in the molten glass was solved assuming two-dimensionality. A further study of this kind has been performed by a study by Novak (1980), in which the combustion chamber flowfield was more carefully estimated with the assistance of empirical data for nonreacting flows for cylindrical ducts. The study of Carvalho and Lockwood (1985) extended the work presented in Carvalho (1983) to an industrial furnace of differing configuration and brought into analysis the batch and glass tank flows assuming two--dimensionality of the batch flow. The glass tank flow predictions were made with a three-dimensional computer procedure.

The present work deals with a completely three-dimensional simulation of an industrial glass furnace, extending the work of Carvalho et al. (1988-b) to the improvement of an industrial glass furnace design. Predictions were made for a wide range of parameters of the combustion chamber, and their effects on the furnace are quantified in a demonstration of the abilities of the procedure. The main feature of the combustion chamber of the predicted furnace, under real operating conditions, was the poor mixing pattern between oxygen and fuel as a consequence of the inlet port design, namely the position of the fuel injector [see Carvalho et al. (1988-b)]. For this reason, there was a small amount of wasted unburned fuel at the outlet. To enhance the combustion chamber performance, several runs were made and the results are presented in this paper. The excess air and preheat levels were varied, and a better position of the fuel injection was sought.

The combustion chamber and the molten glass flow were studied by a cyclical iterative way, by separated calculations, matched by the relation between the heat flux from the flame to the glass surface and its temperature. Assuming known values of the temperature of the glass surface, the flow, combustion process, and heat fluxes were predicted by

a three-dimensional solution technique, which forms the
first submodel. Using the calculated heat flux toward the
glass as a boundary condition, the flow and the temperature
distribution of the molten glass were predicted by a differ-
ent three-dimensional numerical technique, which forms the
second submodel. These glass surface temperatures were then
introduced as a boundary condition in the first submodel,
framing a cyclical iterative procedure that "converged"
solution allows one to predict the performance of the whole
furnace.

## B. Description of the Furnace

Figure 1 shows a sketch of the actual glass furnace,
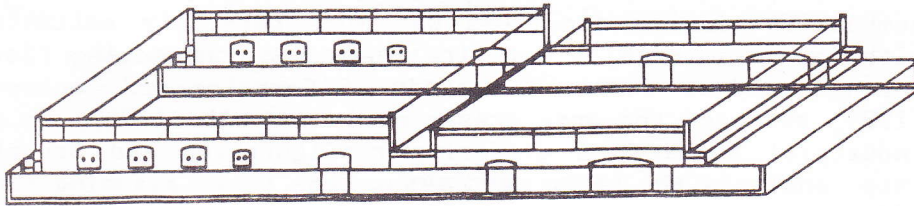which is of the Pittsburgh kind.
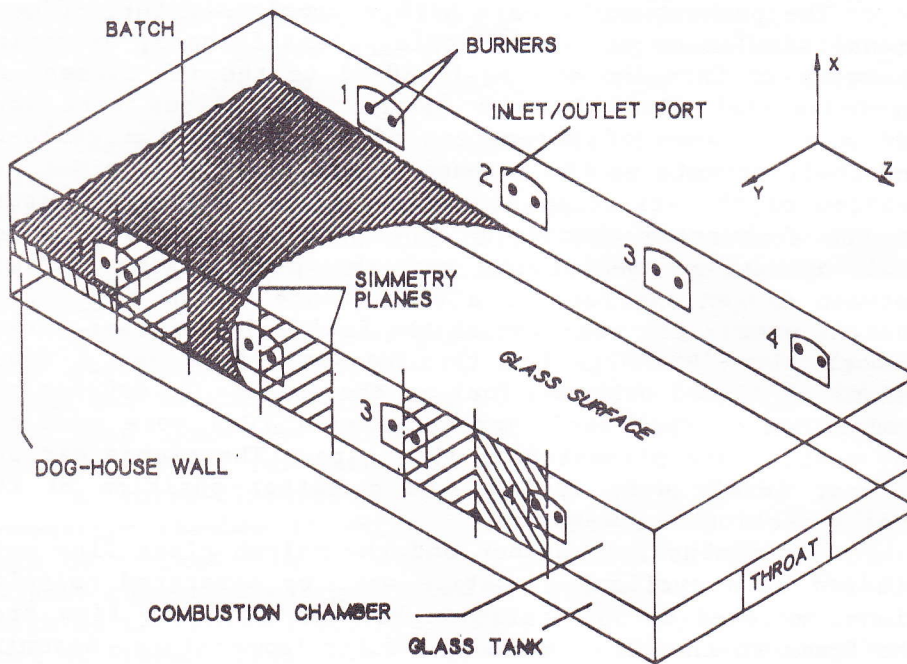


Fig. 1  Sketch of the furnace.



Fig. 2  Calculation domain.

Figure 2 shows a sketch of the furnace region on which the numerical geometry is based, which is essentially a large insulated container in which the batch enters via the doghouse and the molten glass flows from the doghouse near-wall to the opposite endwall. The firing ports are located along the sides of the furnace. There are four ports on each side, each port containing two fuel jets. The furnace is fired alternately from either side to give more uniform heat flux to the glass and to make regeneration possible. The combustion products pass through regenerators that are used to preheat the combustion air before it enters the furnace to produce higher temperatures and heat flux to the glass. Waste ports opposite burners working as outlet ports are demanded by the reversing operating conditions. Heavy oil is burned with excess of air. Upper and side walls of the furnace are refractory-lined.

## II.  The Physical Modeling

The present modeling problem in its entirety has two distinct parts: the simulation of the combustion chamber and the simulation of the glass tank. We have treated these separately, with the aid of different numerical solution procedures. The simulation of the whole furnace is a hybrid treatment involving the two codes. Details of these models can be found in Carvalho et al. (1988-b).

### A. The Combustion Chamber

The governing transport equations for the mean motion of a turbulent three-dimensional reacting flow were applied in their cartesian co-ordinate form.

The Mean Flow Equations. The time-averaged equations for the conservation of momentum were used as well as the equation for the conservation of energy. In addition to the referred equations, one must also include the equation of mass continuity.

The Turbulence Model. The "two-equation" model (Launder and Spalding 1972), in which equations for the kinetic energy of turbulence $k$ and its dissipation rate $\varepsilon$ are solved, was considered appropriated.

The Combustion Model. The combustion model is based on the ideal of a single step and fast reaction between the gaseous fuel and oxidant, assumed to combine in stoichiometric proportion. Equal effective turbulent mass diffusion coefficients for the fuel and oxidant and an instantaneous reaction are also assumed [see Pun and Spalding (1967); Bilger (1980)].

The transport equation for the mixture fraction f was solved.

Furthermore, we have assumed that the chemical kinetic rate is fast with respect to the turbulent transport rate; then fuel and oxidant cannot coexist, so $m_{fu} = 0$ for $m_{ox} \geq 0$ and $m_{ox} = 0$ for $m_{fu} \geq 0$, and the concentrations $m_{fu}$ and $m_{ox}$ are related linearly to the mixture fraction.

The above modeling, it may be noted, presumes a stationary thin-flame envelope. The fluctuating nature of the turbulent reaction is more usually accomodated (e.g., in the work of Spalding 1971) through a modeled equation for the variance of the mixture fraction fluctuations.

We have adopted a statistical approach to describe the temporal nature of the mixture fraction fluctuations. In the present work we have assumed the "clipped normal" probability density function (Lockwood and Naguib 1975), which is characterized by just two parameters: f and the mean square of the f fluctuations $g = \overline{(f - \overline{f})^2}$.

Particular attention was given to radiation because it plays a dominant role in the heat transfer process inside industrial furnaces, and a simple and economical model for oil-fired furnaces was used in which it was assumed that the oil spray evaporates instantaneously.

The Soot Model. The distinctive feature of oil-fired flames is their significant soot content. Soot is of concern because its presence greatly augments the radiation heat transfer and because it is a pollutant. To predict the spacial distribution of soot, a transport equation of its mass concentration was solved. To characterize soot production, a simple global expression similar to that used by (Khan and Greeves 1974) was chosen. A straightforward method of estimating the rate of soot burning proposed by (Magnussen and Hjertager 1976) was used in the present work.

The Radiation Model. The "discrete transfer" radiation prediction procedure of (Lockwood and Shah 1981) was utilized in this study. This method combines ease of use, economy, and flexibility of application. This last feature is of particular importance in the real world of geometrically intricate combustion chambers.

The gas absorption coeficient was calculated from the "two grey plus a clear gas" fit of Truelove (1976). Water vapor and carbon dioxide are the prime contributors to the gaseous radiation.

## B. The Glass Tank

The governing transport equations of the three-dimensional laminar flow driven by free convection were applied in their cartesian co-ordinate form.

The Governing Equations. The conservation of momentum may be written, in tensor notation, as follows:

$$\frac{\partial}{\partial x_j} [\rho u_j u_i + p \delta_{ij} - \mu (\frac{\partial u_i}{\partial x_j} + \frac{\partial u_j}{\partial x_i} - \frac{2}{3} \frac{\partial u_k}{\partial x_k} \delta_{ij})]$$

$$- \rho g_i \beta (T - T_o) = 0 \qquad (1)$$

where $\beta$ is the volumetric coefficient of thermal expansion, and $T_o$ is a reference temperature. The last term of this equation represents the buoyancy term.

The energy equation is

$$\frac{\partial}{\partial x_j} (\rho u_j T) - \frac{\partial}{\partial x_j} (\Gamma_T \frac{\partial T}{\partial x_j}) - S_T = 0 \qquad (2)$$

and the continuity equation is given by

$$\frac{\partial}{\partial x_j} (\rho u_j) = 0 \qquad (3)$$

The property values, varying with temperature, were calculated by special functions, as described below.

The dynamic viscosity was calculated by the Fulcher-Vogel-Tamman equation (Stanek 1977):

$$\mu = \exp(-A + \frac{B}{T - T_o}) \qquad (4)$$

where A, B, and $T_o$ are constants calculated from (COVINA Laboratories 1986).

The density was calculated from the following equation (Stanek 1977):

$$\rho = \rho_o [1 - \beta (T - T_o)] \qquad (5)$$

where $\rho_o$ is the density of the molten glass at the temperature $T_o$.

The radiation transfer was handled by the Rosseland (optically thick) approximation, which results in appropriately augmented thermal conductivities in the energy balance equation. From, the work of Tooley (1974), the thermal conductivity was given by

$$K_{eff} = (C_1)_k T^3 \qquad (6)$$

where $(C_1)_k$ is a constant calculated from a report from COVINA Laboratories (1986).

It was assumed from experimental observation that the batch region, which is a mixture of raw material (sand) and recycled glass, forms a thin layer covering the molten glass from the doghouse (batch inlet door) until the second burner. It was also assumed that the batch temperature varies linearly between the inlet batch temperature and the melting temperature of the batch.


### III.   The Numerical Solution Procedure

## A. Preliminary Considerations

The combustion chamber and the glass tank were simulated separately by different numerical solution procedures used as a hybrid treatment to simulate the whole furnace.

Nearly all industrial furnaces are three-dimensional and exhibit the disparity of scales, in that most of the combustion takes place within a volume surrounding the burner, which occupies only a small proportion of total furnace volume but requires a disproportionately large portion of the total computational grid.

To avoid excessive memory requirement, the combustion chamber is assumed to consist of slices. Each slice is contained between the midway plane of one inlet port and the midway plane between this inlet port and the neighboring one. As shown in Fig. 2, there are four inlet ports with two burners in each one, wich makes eight slices to simulate the whole combustion chamber.

In the work of Megahed (1978), the combustion chamber was divided into several slices, but only two were calculated: the first representing the region over the molten glass and the second simulating the region over the batch. However, in the present case the inlet conditions differ significantly from one port to another (see Table 1), and

Table  1   Inlet conditions

| Port no. (Fig. 2) | 1 | 2 | 3 | 4 |
|---|---|---|---|---|
| Total fuel flow (Kg/h) | 327 | 496 | 496 | 175 |
| Total air flow (Kg/h) | 5480 | 8100 | 8680 | 3810 |
| Excess air (%) | 14 | 11 | 19 | 48 |
| Fuel velocity (m/s) | 0.505 | 0.765 | 0.765 | 0.27 |
| Air velocity (m/s) | 4.23 | 6.34 | 6.70 | 2.94 |

the overall performance of the combustion chamber was ob-
tained by studying four slices (each one containing differ-
ent inlet ports).

   Because of the large period of time between the
changes of side-firing in the furnace, the cycling nature of
the firing process was neglected.

   The glass tank predictions were made for the entire
volume because they did not demand particular refinement of
the grid.

## B. Method of Solution

   The finite difference method used to solve the equa-
tions entails subdividing the combustion chamber and the
tank into a number of finite volumes or "cells." Both sol-
ution algorithms are embodied in versions of TEACH program
(Gosman et al. 1976) for three-dimensional recirculating
flows. The convection terms were discretized by the hybrid
central/upwind method (Spalding 1972).

   In the combustion chamber predictions, the velocities
and pressures are calculated by a variant of the SIMPLE
algorithm described in the work of Caretto et al. (1972).

   In the tank flow predictions, the velocities and
pressure are calculated by a variant of the PISO algorithm
presented by Issa (1982). The use of PISO results in a
substantial reduction in computing effort over that required
by iterative methods (Issa et al. 1983).

   The solution of the individual equations sets was
obtained by a form of Gauss-Seidel line-by-line iteration,
in both submodels.

## IV   Presentation and Discussion of the Results

## A. Some Computational Details

   The present prediction procedure has been applied for
the solution of the process in a full-scale industrial glass
furnace with the real operating conditions. The daily pro-
duction of the glass, or the throughput, is 100 tones.

   As described in Sec. 3, the furnace contains four
firing ports. The total mass flow of fuel and air at each
port can be found in Table 1, which presents the normal
operating conditions of the furnace (designated in the
present work as "RUN 1").

   The fuel is injected at $393^{\circ}$K and the air is pre-
heated to be injected at $1273^{\circ}$K. The fuel composition is 86%
carbon and 14% hydrogen. The inlet axial velocities of fuel

and air can be found on Table 1. The radial and tangential velocities were set to zero due to absence of swirl.

The kinetic energy of turbulence at the inlet $k_{in}$ was assumed to be 0.3% of the kinetic energy of the mean flow, and its dissipation rate ($\varepsilon_{in}$) was calculated from the relation

$$\varepsilon_{in} = \frac{6.0 \, k_{in}^{1.5}}{\ell}$$

where $\ell$ is a characteristic length scale.

Each port operates under different combustion conditions. The excess air can be found at the referred table. These conditions provide a transversal heat flux distribution with a maximum value between the second and the third burner. A given glass temperature distribution, calculated by the glass tank submodel, was used for the furnace combustion chamber predictions.

Part of the upper surface of the molten glass is covered by a batch blanket. Close to this solid surface, the tangential velocity is set to zero due to the nonslipping interface fluid-solid condition. In the remaining part of the referred surface, the velocity is calculated from a vanishing shear-stress condition. A given parabolic profile was used for inlet velocities (Oliveira 1986). For the outlet (glass flowing through the throat channel), streamwise velocity gradients were set to zero. The heat flux, calculated by the combustion chamber submodel, was used to predict the glass tank operating conditions.

Overall heat transfer coefficients were calculated based on the building material thickness and external cooling conditions given by a report from COVINA Laboratories (1986). These values vary from 1.9 to 7.1 $W.m^{-2}.{}^{o}K^{-1}$.

For the combustion chamber predictions a numerical grid comprising 14 x 10 x 14 grid nodes in the x, y, and z co-ordinate directions, respectively, was used, simulating each half-port slice of the furnace, whereas for the whole glass tank predictions a 14 x 16 x 27 grid was used.

Calculations for the whole furnace were made by the following procedure:

1) A slice of the combustion chamber corresponding to one of the half-ports (Fig. 2) was predicted, assuming a glass surface temperature distribution. The results obtained were used as initial values to predict the remaining three half-port slices of the combustion chamber. For RUN 1, 300 iterations were needed [38 central processing unit (CPU) hours in a MicroVax II] to achieve convergence for the first half-port slice (the results were considered converged when

Table 2 The parameters investigated (the values are referred to the third slice of the combustion chamber)

| RUN | Excess air (%) | Air preheating ($^\circ K$) | Burner axis distance from the floor (m) | Investigated parameter |
|---|---|---|---|---|
| 1 | 19 | 1273 | 0.35 | Standard run |
| 2 | 19 | 1373 | 0.35 | The effect of |
| 3 | 19 | 1173 | 0.35 | air preheating |
| 4 | 25 | 1273 | 0.35 | The effect of |
| 5 | 0 | 1273 | 0.35 | the excess air |
| 6 | 19 | 1273 | 0.7 | The position of the fuel jet |

the normalized residuals of the equations were less than $5 \times 10^{-3}$). For the other slices, only 120 iterations (15 CPU hours) were needed.

2) With the fluxes to the glass, calculated from the previous runs, the whole glass tank was predicted, with the same convergence criteria, which takes 120 iterations (13 CPU hours in the same computer).

3) The temperature distribution of the glass surface was then used to repeat the whole process from step 1.

4) The procedure was considered converged when the glass surface temperatures and the fluxes to the glass did not vary by more than 10% from one cycle to the next one. At the end of the fourth cycle "convergence" was achieved.

The conditions described before (see Table 1) were used as the standard run (RUN 1), which defines the operating conditions of the furnace. This study was directed toward the improvement of the actual design and operating conditions of the furnace. Several runs were made for an optimization of the combustion chamber operating conditions. The effect of operating conditions such as excess air and preheat were studied, and the best position of the fuel jet was sought. Table 2 shows a summary of the parameters under investigation.

## B. Discussion of the Results

Validation of furnace predictions against experimental data acquired in a full-scale industrial glass furnace with the real operating conditions is a very important task. In spite of that, measurements are very uncommon because it is difficult to obtain them due to severe conditions of high

temperature and corrosion levels occurring inside the fur-
naces.

A few outlet data values are given in a report by
COVINA Laboratories (1986) and are compared with the pre-
dicted values in Table 3.

As can be seen, the predicted values do agree quite
well with the very few experimental ones. In spite of the
lack of good quantitative validation evidence, the trends in
the results show that the performance of this furnace is
well-characterized by the mathematical model. In the numeri-
cal treatment of this furnace, some sources of inaccuracy
may be presented. The interaction between two neighboring
flames is neglected. The application of the hybrid cen-
tral/upwind scheme may lead to numerical diffusion. The
sources of error together with the simplicity of the turbu-
lence and combustion model have proved to be minor in previ-
ous application (Carvalho et al. 1988-a). Indeed, the com-
bustion chamber models used herein are the same as those
used by Carvalho et al. (1988-a), where extensive validation
of the predictions against experimental data acquired in a
real furnace were made. The results have shown good agree-
ment between both. This is a consequence of the importance
of the radiation in large industrial furnaces.

Table   3   Outlet port no. 3 data (RUN 1)

| Variable | Experimental values | Predicted values |
|---|---|---|
| Outlet velocity (m/s) | 8.30 | 8.60 |
| Outlet temperature ($^\circ$K) | 1720 | 1710 |
| Outlet $CO_2$ mass concentration | 0.14 | 0.15 |
| Outlet $O_2$ mass concentration | 0.034 | 0.04 |

Table   4   Predicted performance criteria of the furnace

| RUN | Energy input (KW) | | | Total heat flux to the glass (KW) | Outlet temperature ($^\circ$K) |
|---|---|---|---|---|---|
| | Air | Fuel | Total | | |
| 1 | 1596 | 2826 | 4422 | 980 | 1710 |
| 2 | 1720 | 2826 | 4546 | 1032 | 1865 |
| 3 | 1470 | 2826 | 4296 | 831 | 1790 |
| 4 | 1797 | 2826 | 4623 | 940 | 1840 |
| 5 | 1436 | 2826 | 4262 | 925 | 1817 |
| 6 | 1596 | 2826 | 4422 | 983 | 1720 |

Table 4 illustrates some aspects of the comparative study of the combustion chamber performance for the parameters under investigation. Figures 3 to 6 show, respectively, the temperature distribuition and fuel, oxygen, and carbon dioxide concentrations for each run on the vertical plane containing the burner and normal to the inlet/outlet port. Figure 7 shows the fuel concentration on the nearest plane parallel to the outlet port, which is the last plane calculated by the model. The effects on the furnace of varying the air preheat and excess air levels, relative to the actual conditions (RUN 1), are described below.
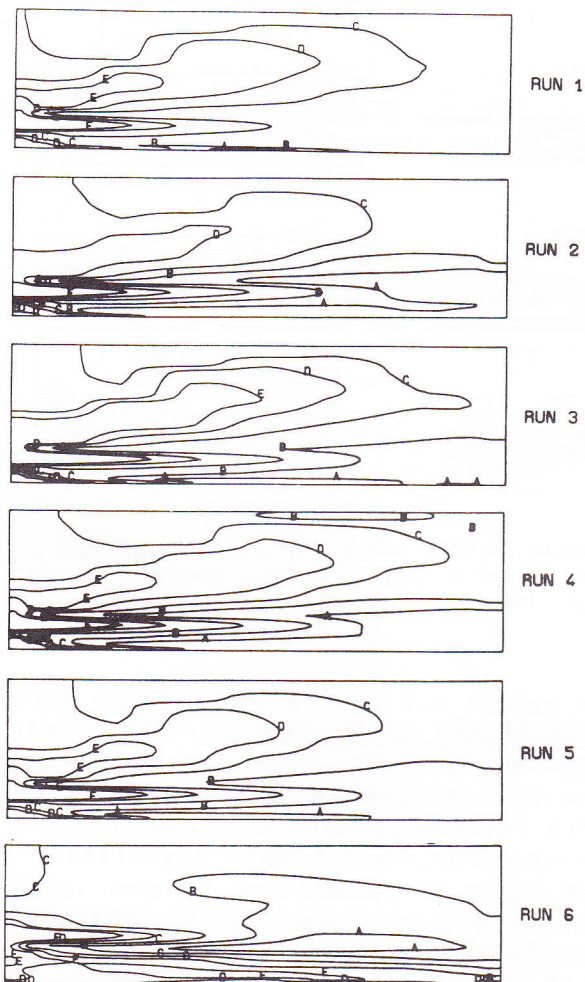


Fig. 3   Temperature distribution (°K) for all studied cases (combustion chamber; Z=0.43 m): A=1880, B=1800, C=1650, D=1450, E=1300.

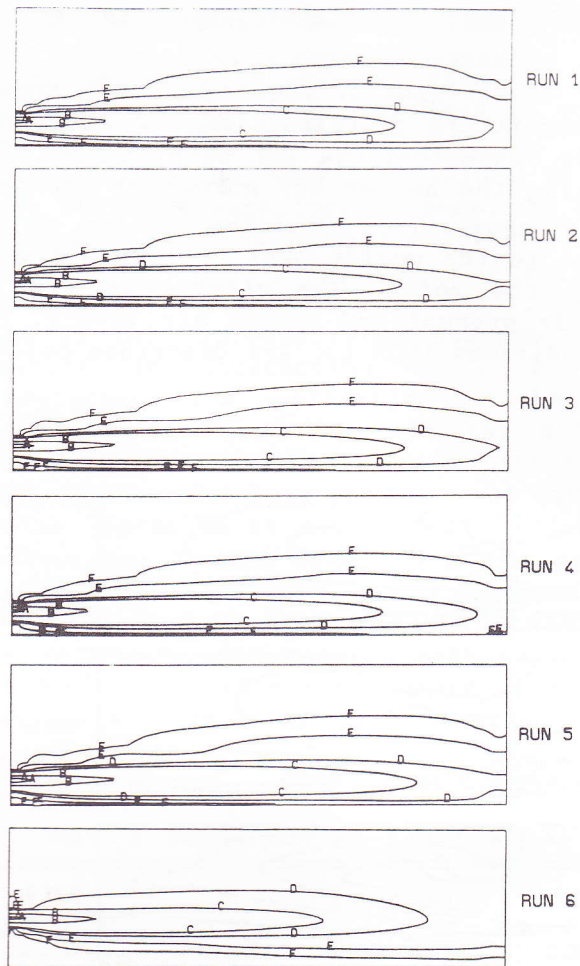Fig. 4  Fuel mass concentration for all studied cases (combustion
        chamber;  Z=0.43 m):  A=0.80,  B=0.50,  C=0.10,  D=0.05,
        E=0.008, F=0.0005.


1. Effect of the Air Preheating. The effect of the air
preheating can be seen by comparing cases 1, 2, and 3.
Increasing the air preheat to $1373^{\circ}K$ (RUN 2) increases the
gas temperature field (Fig. 3). The fuel, oxygen, and carbon
dioxide concentrations do not vary significantly, as shown
by Figs. 4 to 6. As a consequence of the higher levels of
the gas temperature, the total heat flux to the glass
increases (see Table 4) as well as the outlet temperature.
The decrease of air preheat to $1173^{\circ}K$ (RUN 3) decreases the
gas temperatures inside the combustion chamber. Figure 7
shows that the level of air preheat does not influence
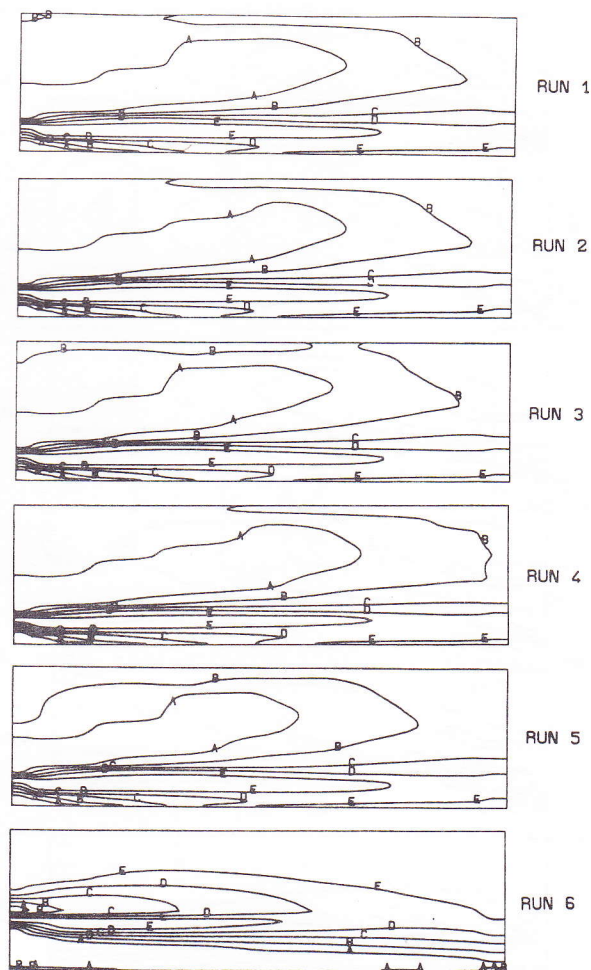significantly the wasted unburned fuel at the outlet.

Fig. 5  Oxygen  mass  concentration  for  all  studied  cases
(combustion  chamber;  Z=0.43  m):  A=0.20,  B=0.15,  C=0.10,
D=0.06, E=0.02.

2. Effect of the Excess Air. The effect of the excess
air can be determined by comparison of cases 1, 4, and 5.
Both the increase of the excess air to 25% (RUN 4) and the
decrease to the stoichiometric proportion (RUN 5) lead to a
reduction of the total heat flux to the glass (Table 4) and
an increase of the outlet temperature. Figures 4 to 6 show
that the fuel, oxygen, and carbon dioxide concentrations
have no qualitative differences. However, the wasted un-
burned fuel varies indirectly proportional with excess air
in both RUN 4 and RUN 5, as shown by Fig. 7. The temperature
levels inside the combustion chamber are higher for RUN 4
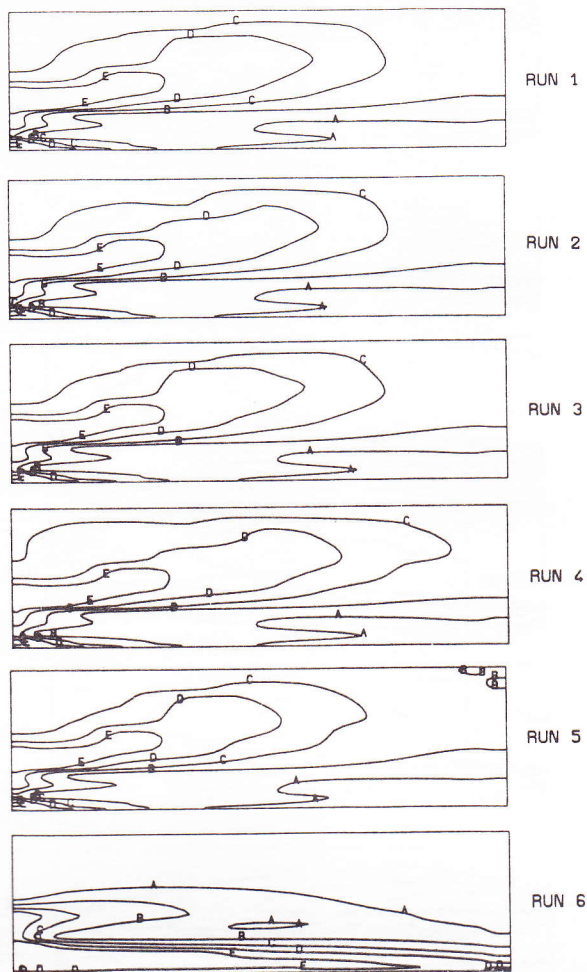due to a more efficient combustion (Fig. 3).

Fig. 6  Carbon dioxide mass concentration for all studied cases
        (combustion chamber; Z=0.43 m): A=0.15, B=0.10, C=0.06,
        D=0.03, E=0.01.

The results described above confirm the poor mixing
pattern between oxygen and fuel in the present geometry.
Figure 5 shows that, in the cases observed (RUN 1 to RUN 5),
there is a considerable amount of unused oxygen in the upper
region of the furnace, where there is no fuel (Fig. 4), and
some unburned fuel leaves the furnace (Fig. 7). A better
performance of the furnace was sought by changing the fuel
injection position.

    3. Effect of the Position of the Fuel Jet. The influ-
ence of the position of the fuel jet on the resulting flow
and temperature fields and mass fraction distributions can
be assessed by comparing RUN 1 with RUN 6. For RUN 6, the
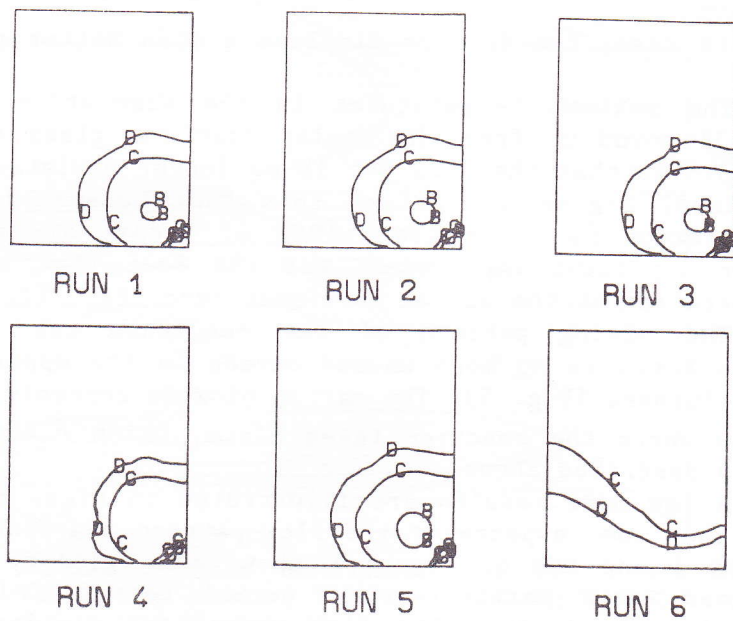fuel injection distance to the glass surface was duplicated.

RUN 1        RUN 2        RUN 3

RUN 4        RUN 5        RUN 6

Fig. 7  Fuel mass concentration for all studied cases at the outlet port (combustion chamber; Y=7.00 m): B=0.05, C=0.005, D=0.0005.



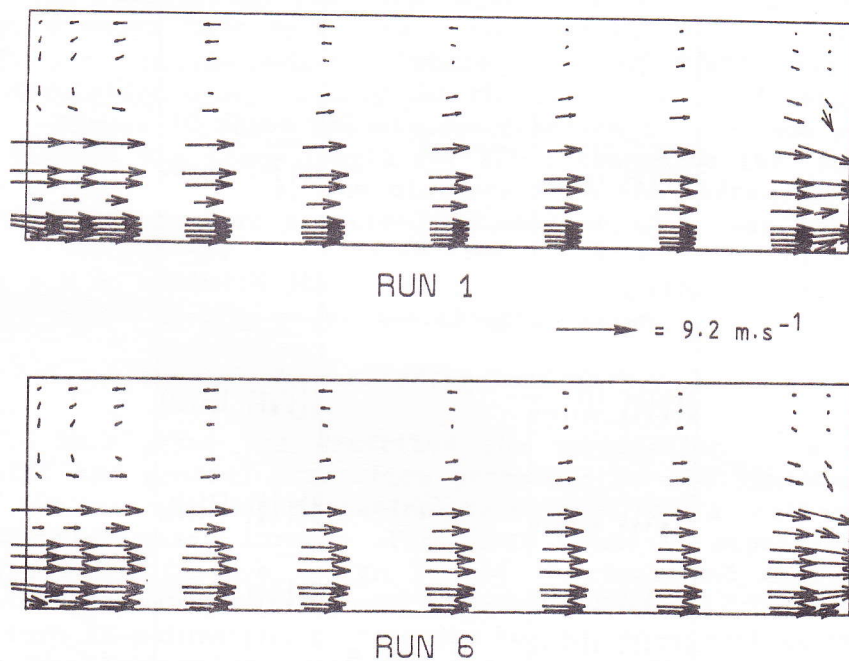RUN 1

$\longrightarrow = 9.2\ m.s^{-1}$



RUN 6

Fig. 8  Velocity vectors for RUN 1 and RUN 6 (combustion chamber; Z=0.43 m).

For this case, the furnace displays a much better perform-
ance.

The maximum temperatures in the combustion chamber
(Fig. 3) moved up from the region near the glass surface,
which proves that the fuel jet is no longer deviated toward
the glass. Figure 4 confirms this fact because the fuel
concentration near the glass (RUN 6) became almost zero.
Another important improvement was the fact that the fuel
concentration at the outlet is almost zero (Fig. 7).

The mixing pattern of the reactants was improved
because there is no more unused oxygen in the upper region
of the furnace (Fig. 5). The carbon dioxide concentration is
maximum where the reaction takes place, which confirms the
results described above.

A few more results are illustrated in Figs. 8 to 10,
which show some aspects of the flow pattern and flame shape
for RUN 1 and RUN 6. Figure 8 shows the velocity vectors
projected on a vertical plane normal to the inlet port
containing the burner. The flow pattern is similar, apart
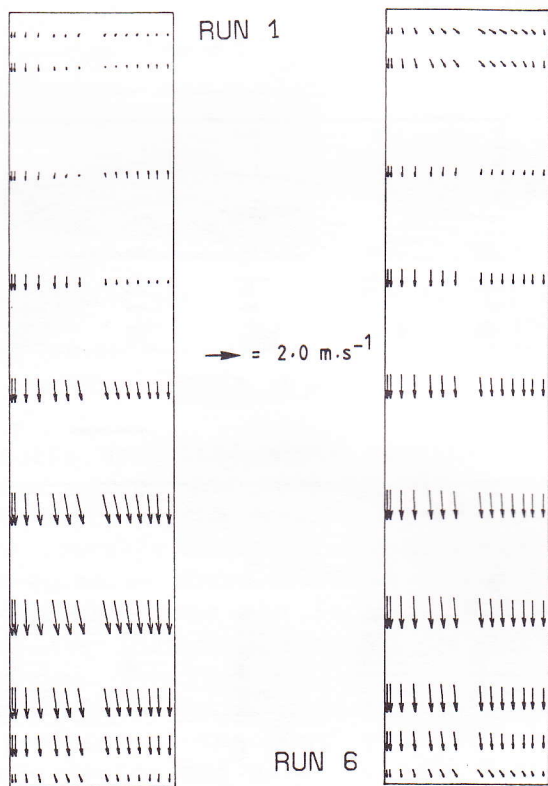from the different location of the fuel injection.



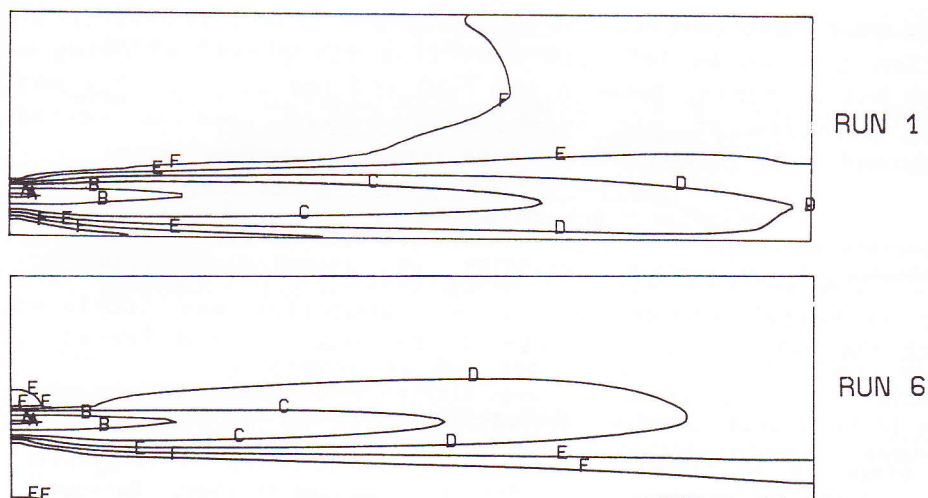Fig. 9   Velocity vectors for RUN 1 and RUN 6 (combustion chamber;
         X=1.90 m).

Fig. 10  Mixture  fraction  distribution  for  RUN  1  and  RUN  6
         (combustion  chamber;  Z=0.43 m):  A=0.80,  B=0.50,  C=0.20,
         D=0.10,  E=0.05,  F=0.025.


Figure  9  shows  the  flow  in  the  horizontal  plane  near
the  roof  of  the  furnace.  The  upper  recirculation  zone  is
extended  to  the  whole  furnace  in  the  case  of  RUN  6  as  the
flow  is  inverted  in  its  total  width  and  length.  For  RUN  1,
Fig.  9  shows  that  this  total  invertion  occurs  only  in  the
left  part  of  the  furnace,  whereas  in  the  right  half  the
recirculation  occupies  only  two  thirds  of  the  total  length.

Figure  10  shows  the  mixture  fraction  in  the  same  plane
as  Fig.  8.  The  flame  length  for  RUN  6  (based  on  the  "chemi-
cal  definition,"  i.e,  the  distance  from  the  burner  of  sto-
ichiometric  mixture  fraction)  is  smaller  than  that  for  RUN
1.  Values  for  the  flame  length  for  RUN  6  and  RUN  1  of  6.2 m
and  6.8 m,  respectively,  were  predicted  against  a  value  of
6.5 m  obtained  from  experimental  observation.

## V. Concluding Remarks

This  paper  has  described  the  application  of  a  very
useful  and  general  prediction  procedure  to  the  improvement
of  the  design  and  operating  conditions  of  a  full-scale
industrial  glass  furnace.  From  this  study  it  appears  that
the  present  furnace  design  is  not  the  best  and  that  many
improvements  can  be  achieved  with  minor  changes.  The  mixing
pattern  is  not  very  efficient  due  to  the  inlet  port  geometry
and  the  combustion  chamber  aerodynamics.  The  cross-stream
velocities  around  the  fuel  jet  are  directed  in  such  a  way  to
carry  the  fuel  away  from  air  and  toward  the  glass.  The
change  of  the  fuel  jet  position,  as  made  in  RUN  6,  prevents

this phenomena because the low pressure inside the recirculation zone pulls the fuel away from the glass, allowing a much better mixing between the fuel and the air. In this way the usability of air input is increased, and no wasted unburned fuel leaves the furnace.

## Acknowledgments

The authors wish to acknowledge COVINA Laboratories for technical advice. The final manuscript was completed with the help of M. Cristovão, F. Farinha, and Rui Ferreira.

## References

Bilger, R. W. (1980) Turbulent flows with non-premixed reactants, turbulent reacting flows. Topics in Applied Physics, Springer-Verlag, Berlin, FRG. (edited by P. A. Libby and F. A. Williams).

Caretto, L. S., Gosman, A. D., Patankar, S. V., and Spalding, D. B. (1972) Two calculation procedures for steady, three-dimensional flows with recirculation. Proceedings of the Third International Conference on Numerical Methods in Fluid Dynamics, p. 60. Springer-Verlag, New York.

Carvalho, M. G. (1983) Computer simulation of a glass furnace, Ph.D. Thesis, University of London, UK.

Carvalho, M. G., Durão, D. F. G., Heitor, M. V., Moreira A. L. N., and Pereira, J. C. F. (1988-a) The flow and heat transfer in an oxy-fuel glass furnace. First European Conference on Industrial Furnaces and Boilers, Lisbon, Portugal.

Carvalho, M. G., Durão, D. F. G., and Pereira, J. C. F. (1987) The prediction of the flow, reaction and heat transfer in an oxy-fuel glass furnace. Int. J. Comput. Aided Eng. Software, 4, 23-31.

Carvalho, M. G. and Lockwood, F. C. (1985) Mathematical simulation of an end-port regenerative glass furnace. Proc. Inst. Mech. Eng., 199, C2, 113-120.

Carvalho, M. G., Oliveira, P., and Semião, V. (1988-b) A three-dimensional modeling of an industrial glass furnace. To be published in J. Inst. Energ.

Chen, T. and Goodson, R. E. (1972) Computation of three-dimensional temperature and convective flow profiles for an elective glass furnace. Glass Technol., 13, 161-167.

COVINA Laboratories (1986) Batch melting and furnace data. Report of COVINA Laboratories, Lisbon, Portugal.

Gosman, A. D., Humphrey, J. A. C., and Vlachos, N. S. (1976) TEACH-3E: A general computer program for three-dimensional

recirculating flows. Report CHT/76/10, Mechanical Engineering Department, Imperial College, London, UK.

Gosman, A. D., Lockwood, F. C., Megahed, I. E. A., and Shah, N. G. (1980) "The prediction of the flow reaction and heat transfer in the combustion chamber of a glass furnace", AIAA Paper-80-0016, AIAA 18th Aerospace Sciences Meeting, CA.

Issa, R. I. (1982) The solution of fluid flow equations operator splitting. Report No FS/82/15, Mechanical Engineering Department, Imperial College, London, UK.

Issa, R. I., Gosman, A. D., and Watkins, A. P. (1983) The computation of compressible and incompressible recirculating flows by a non-iterative implicit scheme. Report FS/83/8, Mechanical Engineering Department, Imperial College, London, UK.

Khan, I. M. and Greeves, G. (1974) A method for calculating the formation and combustion of soot in diesel-engines. Heat Transfer in Flames, Scripta Book Co. (edited by N. H. Afgan and S. M. Beer) pp. 391-402.

Launder, B. E. and Spalding, D. B. (1972) Mathematical Models of Turbulence. Academic, New York.

Lockwood, F. C. and Naguib, A. S. (1975) The prediction of the fluctuations in the properties of free, round jet, turbulent diffusion flame. Combust. Flame, 24, 109.

Lockwood, F. C. and Shah, N. G. (1981) A new radiation solution method for incorporation in general combustion prediction procedures. Eighteenth Symposium (International) on Combustion, The Combustion Institute, Pittsburgh, PA.

Magnussen, B. F. and Hjertager, B. H. (1976) On mathematical modeling of turbulent combustion with special emphasis on soot formation and combustion. Sixteenth Symposium (International) on Combustion, The Combustion Institute, Pittsburth, PA.

Mase, H. and Oda, K. (1980) Mathematical model of glass tank furnace with batch melting process. J. Non-Cryst. Solids, 38, 39, 807-812.

McConnell, R. R. and Goodson, R. E. (1979) Modeling of glass furnace design for improved energy efficiency. Glass Technol., 20, 100-106.

Megahed, I. E. A. (1978) The prediction of three-dimensional gas--fired combustion chamber flows. Ph.D. Thesis, University of London, UK.

Novak, J. D. (1980) Application of combustion space energy calculations to commercial glass furnaces. J. Non-Cryst. Solids, 38, 39, 819-824.

Oliveira, P. J. (1986) Convecção natural: um estudo numérico. Aplicação ao escoamento do vidro num forno tanque. M.Sc. Thesis, University of Lisbon, Portugal.

Pun, W. M. and Spalding, D. B. (1967) A procedure for predicting the velocity and temperature distributions in a confined steady, turbulent, gaseous diffusion flame. Proceedings of the International Astronautical Federation Meeting, Belgrade, Yugoslavia.

Semião, V. S. (1986) Simulação numérica de uma fornalha industrial. M.Sc. Thesis, University of Lisbon, Portugal.

Spalding, D. B. (1971) Concentration fluctuations in a round turbulent free jet. Chem. Eng. Sci., 26, 96.

Spalding, D. B. (1972) A novel finite difference formulation for differential expressions involving both first and second derivates. Int. J. Numer. Methods Eng., 4, 557.

Stanek, J. (1977) Electric Melting of Glass. Elsevier, Amsterdam, The Netherlands.

Suzuki, J. (1976) Three-dimensional flow and temperature distributions in rectangular cavities. M.Sc. Thesis, University of Sheffield. UK.

Tooley, F. V. (1974) The Handbook of Glass Manufacture, Vol. 1, Books for Industry.

Truelove, J. S. (1976) A mixed grey gas model for flame radiation. AERE Harwell Report HL 76/3448/KE, Atomic Energy Authority, Oxfordshire, UK.